Modeling, Simulation and Control of a Multi-Copter Endowed with Vectoring Thrust Mechanism

Felipe Machini Malachias Marques[a], Roberto Mendez Finzi Neto, Leonardo Sanches[b]

[a]*Federal University of Uberlândia, Faculty of Mechanical Engineering, Uberlândia, MG, Brazil*
[b]*ISAE- SUPAERO Institut Supérieur de l'Aéronautique et de l'Espace, Toulouse, France*

Abstract

In general, standard multi-copters are classified as an underactuated system since their number of control inputs are insufficient to allow position and orientation tracking independently. Many authors have proposed novel multi-copter designs containing vectoring thrust mechanisms, consequently introducing more control inputs to the model. However, its impact on system performance, especially in trajectory tracking operations, is neglected. In this context, this paper deals with the dynamical modeling of a tilting rotor multi-copter aerial vehicle capable of two different tilting movements (laterally and longitudinally) and the design of a trajectory tracking controller using modern control techniques. The model is validated using numerical simulations for different tilting configurations aiming the system performance and control behavior analysis. The conclusions has shown that the system endowed with tilting mechanism may have better transient performance but spends more energy to complete the desired mission.

Keywords: Unmanned Aerial Vehicle, Multi-rotor, Tilt-rotor, Modern control, Trajectory tracking.

*Corresponding author
Email address: machini@ufu.br (Felipe Machini Malachias Marques)

1. Introduction

Multi-rotor helicopters are included in the category of vertical take-off and landing (VTOL) unmanned aerial vehicles (UAVs) having more than two motor-propulsive set. In the past few decades UAVs has been considered a turning point compared to manned aerial vehicles, considering safety and cost, once they dismiss a pilot on board. As a consequence they can avoid human lives risks and favor aircraft miniaturization specially for autonomous operations in short range and restricted space. Hence, a new UAV category has gained prominence on the global market which are the Micro Aerial Vehicles (MAVs) [1].

On the control point of view, since multi-copter MAVs are considered as open-loop unstable systems, it becomes indispensable the design of a control law so it can operate , either autonomously or remotely, on safe conditions. The control design challenges for MAVs has attracted the attention of researchers on recent years due to their mechanical simplicity, simple dynamics and low cost, making them the ideal robotic platforms for the development and testing of control strategies [2].

In general, standard multi-rotor UAVs are equipped with propulsive set attached to its structure which generates the required thrust force to maintain the system airborne. The number of rotors establishes the resulting thrust force and, consequently, the payload capacity of the MAV, but also affects stability and controllability of the system. Moreover, for this configuration, position and attitude control are coupled since they are based on the propeller angular speed variation of each rotor independently. Fixed rotor multi-copters, specially quad-rotors, has been the research object for many control design studies, either linear or non-linear [3, 4, 5, 6, 7, 8, 9, 10].

However, as discussed in [11], attitude and position cannot be controlled independently on fixed rotor configurations since they are classified as underactuated systems, i.e. the number of input commands is lower than the number of controlled states. Hence, in this scenario, the rotorcraft is only capable to perform hovering flights when the roll and pitch attitude angles are zero, indicating

that the aircraft has only one equilibrium point which is holding an horizontal position w.r.t the inertial coordinate frame.

In this manner, many authors have proposed different mechanical actuation designs in order to optimize the multi-rotor control actuation, enhance controllability, maneuverability and solve the underactuation issue. For instance, on their work, [12] proposed an actuation system where the propeller blades are able to change their pitch angle, similarly to the conventional helicopters. According to them, the variable pitch propellers compared to the fixed configuration could reduce the control effort, have better maneuver agility and the rotors were less susceptible to saturation on aggressive maneuvers. Another actuation strategy is the tilt-rotor mechanism which consists on the rotor rotation w.r.t. the multi-rotor's arm. Therefore, the produced thrust can be vectored, i.e. the thrust force vector can oriented on a desired direction using the tilting mechanisms. The main benefit is that the novel actuation feature can be used for attitude and position control decoupling, allowing the rotorcraft to hover on a non-horizontal position (w.r.t inertial coordinate frame) or/and shift its position without changing its orientation. As examples, [13], [14] and [15] considers a quadrotor UAV whose rotor set axes rotate laterally about the arm longitudinal axis using actuators attached on the arm's extremity. Similarly, [16] presents a quadcopter configuration for narrow path missions composed by 8 rotors installed coaxially two by two allowing the central body to rotate freely using only one actuator. Thus, this multi-copter configuration enables the system operate on hover conditions with different attitude positions.

Further, other works proposes a tilt mechanism where the motor set is capable of tilting longitudinally w.r.t. the multi-copter arm [17, 11]. Equivalently to the lateral ones, the longitudinal tilt mechanism can work in pairs or use one independent actuator for each multi-copter arm. Considering the vectoring capability of the tilting mechanisms (lateral or longitudinal), they can be also used on bi-copters [18] and tri-copters configurations [19, 20] to guarantee stability and allow the MAV to be controlled and perform autonomous flight.

On regarding the state of art of tilt rotor multi-copters presented lately, few

investigations were conducted concerning the dynamical and performance impact of the tilt mechanism addition on the system. Hence, this present work aims to further investigate the dynamical behavior of the proposed tilting mechanisms, either longitudinal or lateral, enhancing the benefits and disadvantages when equipping the system with a thrust vectoring mechanisms. As a consequence, the proposed method can be useful for novel multi-copter analysis and design.

In order to accomplish its objectives, the paper presents the following contents: firstly, a generic dynamical model for tilting rotor multi-copters is developed, considering different structural and tilting mechanism configurations; secondly, to guarantee trajectory tracking capability, a feedback control law based on modern control techniques is proposed assuming random input signals represented by differential equations; lastly, the system is simulated for different signal inputs and actuation configurations comparing the system transient response and actuation effort emphasizing stability and control performance when the MAV is endowed with tilting mechanisms.

2. Dynamic Modeling

The dynamical model of a generic multi-copter equipped with a tilting mechanism is derived in this section using Newton-Euler formulation. For such approach, it is considered that each rotor is capable of tilting in two different directions (laterally and longitudinally with respect to the rotors arm) introducing more control inputs to the system. Some considerations regarding the UAV must be taken before the model development such as: the multi-copter structure and propellers are supposed to be rigid, all the rotors, propeller blades and tilting mechanism equipped are the same.

2.1. Kinematic Relations

For dynamical modelling of the aircraft endowed with the tilting rotor mechanism, three different reference frames are used as illustrated on Fig. 1. The

first, an Earth fixed Inertial Reference System frame denoted by $ICS : \{O_E; x_E; y_E; z_E\}$ is used to represent the absolute position of the aircraft on space. Secondly, a body fixed coordinate frame, represented by $BCS : \{O_B; x_B; y_B; z_B\}$, attached to the aircraft, capable of translating and rotating with the MAV. The origin of the body fixed reference frame coincides with the aircraft center of gravity (CG), and its linear and angular velocity vectors are denoted by $\vec{v} = [u, v, w]^T$ and $\vec{\omega} = [P, Q, R]^T$, respectively, such that P , Q and R are the angular velocities around the x_B, x_B and z_B axis.

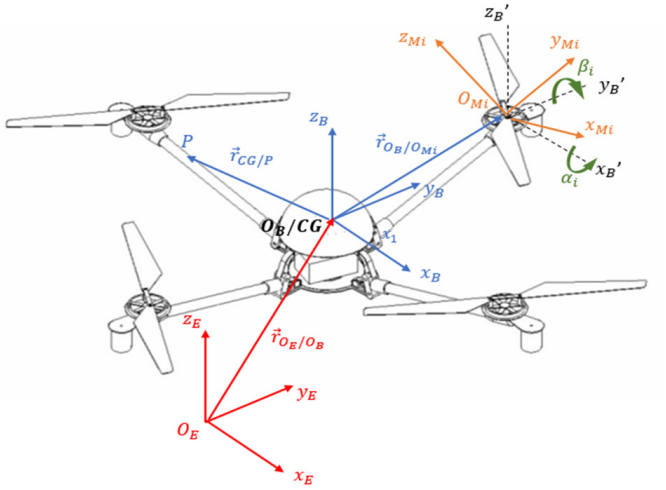

Figure 1: Multi-copter ICS, BCS and MCS axes configuration.

The aircraft attitude or the kinematic relation between the ICS and BCS can be defined with respect to the using the Euler angles notation, which are represented by $\vec{\Theta} = [\phi\ \theta\ \psi]^T$ corresponding to the roll, pitch and yaw angles, respectively. It must be remarked that $\vec{\omega} \neq \dot{\vec{\Theta}}$ since the $\vec{\omega}$ vector points in the rotation axis direction, while $\dot{\vec{\Theta}}$ only represents the time derivative of the attitude angles. However, these two vectors are correlated by the following kinematic equations [21]:

$$\vec{\omega} = \begin{bmatrix} 1 & 0 & -\sin\theta \\ 0 & \cos\phi & \cos\phi\cos\theta \\ 0 & -\sin\phi & \cos\theta\cos\phi \end{bmatrix} \dot{\vec{\Theta}} \tag{1}$$

Any vector represented on the body-fixed frame ($\vec{r}_{BCS}$) is interrelated with the inertial coordinate frame ($\vec{r}_{ICS}$) using Euler angles matrix transformation defined by a rotational matrix (R_B^I) [22].

$$\vec{r}_{ICS} = R_B^I \cdot \vec{r}_{BCS} \tag{2}$$

with $R_B^I = R_B^I(\psi)R_B^I(\theta)R_B^I(\phi)$, being $R_B^I(\psi)$, $R_B^I(\theta)$ and $R_B^I(\phi)$ rotation matrices around z_E, y_E and x_E axis, respectively.

It must be remarked that the R_B^I matrix considers a sequence of rotations on the following order: yaw (ψ), pitch (θ) and roll (ϕ). Since R_B^I is orthogonal, its inverse is equivalent to its transpose. Thus, any vector on the *ICS* can be written on the *BCS* by multiplying $\{R_B^I\}^T$ and the body-coordinate vector ($\vec{r}_{BCS}$).

The motor reference frame MCS: $\{O_{Mi}; x_{m_i}, y_{m_i}, z_{m_i}\}$, $i = 1 \ldots n$ illustrated on Fig.1 is associated to each of the i^{th} propulsive set, with x_{m_i} and y_{m_i} representing the lateral and longitudinal tilting actuation axes, respectively. The z_{m_i} axis is normal to the propeller disc spinning plane and is coincident with the produced thrust force direction [13]. The vectoring rotors are located at the extremities of the UAV's arms at point P_i by an angle $\gamma_i = \frac{\pi}{n}(2i-1)$, $i = 1...n$ w.r.t the x_B axis direction of the *BCS*. Also, similarly as the kinematic relations between the BCS and ICS as function of the aircraft attitude (Euler angles), once the *MCS* translate with the aircraft, the orientation of the *i-th* propeller can be represented on the *BCS* using the following rotation matrices:

$$R_M^B(\gamma_i) = \begin{bmatrix} \cos\gamma_i & -\sin\gamma_i & 0 \\ \sin\gamma_i & \cos\gamma_i & 0 \\ 0 & 0 & 1 \end{bmatrix} \tag{3}$$

$$R_M^B(\alpha_i) = \begin{bmatrix} \cos\alpha_i & 0 & \sin\alpha_i \\ 0 & 1 & 0 \\ -\sin\alpha_i & 0 & \cos\alpha_i \end{bmatrix} \tag{4}$$

$$R_M^B(\beta_i) = \begin{bmatrix} 1 & 0 & 0 \\ 0 & \cos\beta_i & -\sin\beta_i \\ 0 & \sin\beta_i & \cos\beta_i \end{bmatrix} \tag{5}$$

where α_i and β_i represents the longitudinal and the lateral tilt angles about x_{m_i} and y_{m_i}, respectively.

The rotation matrix R_M^B gives the coordinate transformation from MCS to BCS and is composed by the multiplication of Eqs. (3), (4) and (5).

2.2. Equations of Motion

The multi-rotor equations of motion are derived using the Newton-Euler formulation for a six degrees of freedom rigid body system. Thus, the equations for linear and angular body motion, written on the BCS, can be represented by:

$$\sum = m\vec{a} \;\rightarrow\; \begin{bmatrix} \sum F_x \\ \sum F_y \\ \sum F_z \end{bmatrix} = m \begin{bmatrix} \dot{u} - Rv + Qw \\ \dot{v} - Pw + Ru \\ \dot{w} - Qu + Pv \end{bmatrix} \tag{6}$$

$$\sum \vec{M} = \frac{d\vec{H}}{dt} \begin{bmatrix} \sum M_x \\ \sum M_y \\ \sum M_z \end{bmatrix} = \begin{bmatrix} I_{xx}\dot{P} + QR\,(I_{zz} - I_{yy}) - I_{yz}(\dot{R} + PQ) \\ I_{yy}\dot{Q} + PR\,(I_{xx} - I_{zz}) + I_{xz}(P^2 + Q^2) \\ I_{zz}\dot{R} + PQ\,(I_{yy} - I_{xx}) + I_{xy}(QR + \dot{P}) \end{bmatrix} \tag{7}$$

where $\vec{F} = \begin{bmatrix} F_x & F_y & F_z \end{bmatrix}$ and $\vec{M} = \begin{bmatrix} M_x & M_y & M_z \end{bmatrix}$ are the external force and moment applied at the center of mass of the vehicle. I_{xx}, I_{yy} , I_{zz}, I_{xy}, I_{yz} and I_{xz} are the components of the rotational inertia matrix of the vehicle with respect to the body coordinate frame.

2.3. Forces and Moments

Concerning the external forces, it is mainly composed of thrust, drag and gravitational. Assuming that the most commonly type of propulsion system used for UAVs are electric DC motors, the thrust force generated by the propeller is assumed as proportional to the propeller angular speed [23]:

$$T = \left(\frac{K_\tau K_v \sqrt{2\rho\pi r_{prop}^2}}{K_t} \, \Omega \right)^2 = k\Omega^2 \tag{8}$$

with K_t a proportional constant relating the torque produced by the electric motor and its electrical current, K_v relates the motor voltage and its angular velocity, K_τ is relative to the motor torque and thrust, r_{prop} is the blade disc radius, ρ the density of the surrounding air and Ω the angular speed of the motor shaft.

Once the thrust T acts in the z direction of the MCS, the force generated by each rotor can be written in the BCS using the transformation matrix R_M^B on Eq.(2), which results:

$$\vec{F}_T^{BCS} = \begin{bmatrix} \sum_{i=1}^{n} (\sin(\gamma_i)\sin(\beta_i) + \cos(\gamma_i)\sin(\alpha_i)\cos(\beta_i))k\Omega_i^2 \\ \sum_{i=1}^{n} (-\cos(\gamma_i)\sin(\beta_i) + \sin(\gamma_i)\sin(\alpha_i)\cos(\beta_i))k\Omega_i^2 \\ \sum_{i=1}^{n} \cos(\alpha_i)\cos(\beta_i)k\Omega_i^2 \end{bmatrix} \tag{9}$$

The drag force is due to the viscous interaction of the vehicle with the surrounding air and can be simplified by expressing this force as being proportional to the linear velocity of the aircraft and always acting in the opposite direction of the body movement. Hence, the drag force at the BCS is written as:

$$\vec{F}_D^{BCS} = -k_d \vec{v}_B = \begin{bmatrix} -k_{dx} u \\ -k_{dy} v \\ -k_{dz} w \end{bmatrix} \tag{10}$$

where k_d is a friction constant which can be split in three directions of the BCS (x_B, y_B and z_B).

The gravitational force vector is always pointing to the z-direction of the ICS and it is assumed as being constant since the vehicle operates at low altitudes. Its components are obtained using the matrix transformation presented in Eq. (2) using $\{R_B^I\}^T$, as follows:

$$\vec{F}_{grav}^{BCS} = \left(R_B^I\right)^T . \vec{F}_{grav}^{ICS} = \begin{bmatrix} mg \sin\theta \\ -mg \sin\phi \cos\theta \\ -mg \cos\phi \cos\theta \end{bmatrix} \tag{11}$$

The moments acting in the BCS are mainly generated by propeller system actuation and how they are distributed on the UAV center of mass. Hence, the torque produced by the spinning propeller can be expressed as the cross product between the rotor vector position ($r_{CG/P}$) and the thrust force vector (F_T^{BCS}) for each motor set from Eq. (9):

$$\vec{\tau}_T = \vec{d}_i \times \vec{F}_T^{BCS} \tag{12}$$

Afterward, since the mass of the aircraft is generally small, the gyroscopic effect of the blades must be accounted in the dynamic model. This torque is an outcome of the propellers angular momentum direction change along the flight [21], and is calculated with respect to the multi-rotor center of gravity considering the two tilting directions (α_i and β_i). The motor set, when attached to the tilt mechanism, has an angular velocity with respect to the aircraft CG caused by two main phenomenons: the mechanism movement, expressed as the time derivative of the tilt angles $\dot{\beta}_i$, and $\dot{\alpha}_i$ and the aircraft rotation represented by the angular velocity vector $\vec{\omega}$. Hence, the propeller disc angular speed can be written as:

$$\vec{\omega}_{prop} = \begin{bmatrix} \cos(\alpha_i)\dot{\beta}_i + P & \dot{\alpha}_i + Q & -\sin(\alpha_i)\ \dot{\beta}_i + R \end{bmatrix}^T \tag{13}$$

being $\dot{\alpha}_i$ and $\dot{\beta}_i$ each rotor angular velocity rate of change.

Assuming that the propeller blades have the same moment of inertia (I_M) and are spinning around the z_M direction of the MCS, one can state that the angular momentum for each propeller is given by [21]:

$$\vec{H}_{gyro}^{MCS} = \begin{bmatrix} 0 & 0 & \sum_{i=1}^{n} I_{Mi}\Omega_i \end{bmatrix}^T \tag{14}$$

The resultant torque due the propeller gyroscopic effect is obtained from the cross product between the motor angular velocity vector (Eq.(13)) and the angular momentum generated by the propeller described in Eq.(14).

$$\vec{\tau}_{gyro} = \vec{\omega}_{prop} \times \vec{H}_{gyro}^{MCS} \tag{15}$$

Furthermore, the fan torque, which is also an external torque component due to the air aerodynamic drag on the propeller blades cross section that acts

on the rotor spinning axis (z_M), is the actuation torque responsible for the multi-copter's yawning movement. According to [24] it can be modeled as:

$$\overrightarrow{\tau}_{fan}^{MCS} = [0 \quad 0 \quad \sum_{i=1}^{n} -b\Omega_i^2 \ ]^T \tag{16}$$

Thus, in summary, the resultant forces and toques applied to the aircraft are:

$$\vec{F} = \vec{F}_T^{BCS} + \vec{F}_D^{BCS} + \vec{F}_{grav}^{BCS} \tag{17}$$

$$\vec{M} = \vec{\tau}_T + \vec{\tau}_{gyro} + \vec{\tau}_{fan} \tag{18}$$

The mathematical model of a generic tilt multi-rotor with n rotors is obtained substituting Eqs. (17) and (18) in Eqs. (6) and (7) and also considering the kinematic relations presented on Eq. (1) forming a nine state variables dynamical system. The number of inputs depends on the number of motors and tilting actuators.

2.4. State Space Model

In order to apply the modern control techniques proposed in this paper, such as the Linear Quadratic Regulator (LQR), the derived equations of motion must be linearized in order to form a first order derivative LTI (Linear Time Invariant) system state space model which can be written on the state-space format. The procedure of linearization is based on the small perturbation theory similarly to the application of fixed wing aircraft models as developed in [21]. Thus, any state variable can be written as:

$$\xi = \xi_0 + \Delta\xi \tag{19}$$

where $\Delta\xi$ represents the perturbed variable and ξ_0 the equilibrium condition (trim point).

On this case, the hovering flight is set as the equilibrium point, where the Euler angles, linear and angular velocities are zero and, consequently, the approximation is valid only for small perturbations in the surroundings of the trimmed condition.First, the state vector is defined as $\vec{x} = \left\{ \begin{array}{ccccccccc} u & v & w & P & Q & R & \phi & \theta & \psi \end{array} \right\}$ as perturbations of the equilibrium condition. For control purposes, the resultant thrust force (F_z) and the torques on three BCS directions (τ_x, τ_y and τ_z) are considered as the state space input vector $\vec{u}$ whose perturbed approximation, from Eq.(19), is given by :

$$\vec{u} = \vec{u}_0 + \Delta\vec{u} = \begin{bmatrix} F_{z_0} + \Delta F_z \\ \tau_{x_0} + \Delta\tau_x \\ \tau_{y_0} + \Delta\tau_y \\ \tau_{z_0} + \Delta\tau_z \end{bmatrix} \tag{20}$$

Furthermore, the trimming conditions of the aircraft for the hoovering condition are estimated from the equilibrium equations, i.e. the temporal derivative terms are zero on Eqs. (6) and (7). Consequently, the trimmed thrust force and aircraft weight are in equilibrium ($F_{z_0} = F_{T_z}^{BCS} = F_{grav_z}^{BCS}$) while the trimming torques τ_{x_0}, τ_{y_0}, τ_{z_0} are zero.

Once the state variables, forces and moments were linearized considering hoovering condition on Eqs. (6) and (7), the resulting linear first order differential equations can be written in the state space format:

$$\begin{aligned} \dot{\vec{x}} &= A\vec{x} + B\Delta\vec{u} \\ \vec{y} &= C\vec{x} + D\Delta\vec{u} \end{aligned} \tag{21}$$

with $\vec{y}$ being the output measured signals, A the dynamic matrix and B the input matrix. Since the measured signals are considered to be exactly the state vector, then C is an identity matrix and D is a zero matrix. It must be remarked that,for now on, the Δ notation is removed for input perturbed vector ($\Delta\vec{u}$).

In most applications concerning trajectory tracking problems, the position of the aircraft with respect to the *ICS* is the desired control variable [22]. In order to include the vehicle position, the state vector is expanded and three new kinematic relations are added to the set of equations. They concern the linear velocities ($\vec{V}_x$, $\vec{V}_y$ and $\vec{V}_z$) written as a function of the temporal derivatives of (x, y and z) [25].

Once the system is now represented by a linear set of differential equations on state-space format, Modern Control techniques can be applied in order to allow the aircraft to operate autonomously in space.

3. Control Design

The autonomous operation of a multi-copter, by the control point of view, is a challenging task since the open loop system is dynamically unstable. Hence, when concerning trajectory tracking applications, it is common to develop controllers using two main control loops: an internal one, responsible for regulating the angular velocities and attitude to maintain the aircraft on stable flight and an external, used to track the desired position error [10, 8].

Comparing with standard configurations, the addition of the tilting mechanism in the multi-rotor model, as proposed in this work, increases the dynamical complexity once introduces non-linearities and coupling terms to the equation as noted on Eqs. (9), (12) and (13).

Furthermore, on the control design point of view, some simplifications regarding the mechanism operation must be considered [13] as: the motors and actuators actuating the tilting/spinning axis are assumed to have high-gain local imposing the desired angular speeds to the propeller (ω_i) and tilt deflection

($\dot{\alpha_i}$). In other words, one can state that the motor and actuator dynamics can be neglected.

On the other hand, the tilt configuration have some practical benefits as: increasing the number of input signals to the system, such that, it becomes an overactuated system potentially capable of tracking an arbitrary trajectory over time [17]; and increasing mission versatility as the multi-rotor is capable of making roll and pitch maneuvers while hovering in the air and also move horizontally without an inclination angle [11]. Notwithstanding, one may consider that the proposed actuation mechanism have a strict relationship with the system performance, specially for autonomous flight operations, which must be accounted through the multi-copter system design.

3.1. Desired Tilt Angles

In this work, the control law will be designed in such manner that the tilting mechanism actuates in order to keep the thrust vector force always pointing on the z_E direction of the ICS coordinate system, i.e. the trust force produced by the propeller is always in balance with the weight vector.

Thus, one can consider a vector $\vec{r}_p^{\,ICS} = [0 \quad 0 \quad 1]$ representing the direction of the gravitational force vector on MCS, as on Fig. 2. Later, the direction vector can be written on BCS using the matrix transformation from Eq.(2) and, similarly using $\{R_M^B\}^T$ matrix on the same equation, the resulting vector can be represented on MCS considering that $\alpha_i = 0$ and $\beta_i = 0$. Finally, the $\vec{r}_p^{ICS}$ on the motor reference frame is given by:

$$\vec{r}_p^{MCS} = \begin{bmatrix} -\cos\gamma_i \sin\theta - \sin\gamma_i \sin\phi \cos\theta \\ -\sin\gamma_i \sin\theta - \cos\gamma_i \sin\phi \cos\theta \\ \cos\phi \cos\theta \end{bmatrix} \tag{22}$$

Moreover, the tilting angles for each rotor can be obtained from Eq.(22) assuming that the desired longitudinal (α_i) and lateral (β_i) angles can be represented, respectively, by:

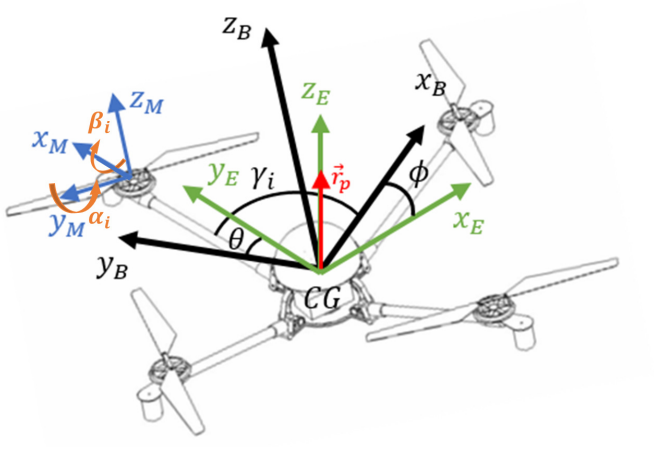

Figure 2: Multi-copter ICS, BCS and MCS axes with respect to the rotors.

$$\alpha_i = \arctan\left(\frac{\sin\gamma_i \sin\phi\cos\theta + \cos\gamma_i \sin\theta}{\cos\phi\cos\theta}\right) \tag{23}$$

$$\beta_i = \arctan\left(\frac{\cos\gamma_i \sin\phi\cos\theta + \sin\gamma_i \sin\theta}{\cos\phi\cos\theta}\right) \tag{24}$$

From Eqs. (23) and (24) one can conclude that the desired tilting angles for each rotor are function of the motor distribution on the $x_b - y_b$ plane and also the aircraft attitude represented by the γ_i angles and the Euler state angles ϕ and θ, respectively. Hence, the desired tilting angles can be estimated from the actual state vector $\vec{x}$ for each time step.

3.2. Modern Control

In terms of autonomous systems development, modern control theory has revealed to be valuable for different mission conditions as presented in [2], [3] and [26]. Large numbers of control states and inputs in the multi-copter dynamical

model make classical control techniques as PID controllers a hard-working task since the controller is based on successively closed loops. Moreover, for multi-variable or *MIMO* (Multiple Input Multiple Output) problems, modern control techniques can be more efficient [27].

Therefore, in this work, the Linear Quadratic Regulator (LQR) with state feedback is applied to guarantee stability and good signal tracking capability. The LQR strategy control strategy consists in making zero order closed loop system that forces all the states to the equilibrium position. Mainly concerned with trajectory tracking characteristics, the tracking error ($\vec{e}(t)$) is defined as:

$$\vec{e}(t) = \vec{r}(\mathrm{t}) - \vec{\mathrm{x}}(\mathrm{t}) \tag{25}$$

being $\vec{r}(\mathrm{t})$ the tracking command vector containing the reference values for the states desired to be tracked which can be represented as a p order time differential equation:

$$\overset{(p)}{r} = \sum_{i=1}^{p} a_i \overset{p-i}{r} \tag{26}$$

Furthermore, the LQR problem can be extended to the LQT (*Linear Quadratic Tracking*) problem increasing the system order following the internal model principle, where the error (Eq.(25)) is driven to zero. The problem can be treated as a servomechanism design which contains the reference model equation (Eq.(26)) written in the state space form as [28]:

$$\dot{\vec{z}} = \tilde{A}\vec{z} + \tilde{B}\vec{\mu} \tag{27}$$

where the vector μ represents the plant input vector and z is the expanded state vector containing the plant and p error derivatives ($\dot{\vec{z}} = \begin{bmatrix} e & \dot{e} & \cdots & e^{(p-1)} & x \end{bmatrix}^T$). Further, assuming that the control law is represented by:

$$\vec{\mu}(t) = -K_c \vec{z} \tag{28}$$

The feedback gain $K_c = \begin{bmatrix} K_p & K_{p-1} & \cdots & K_1 & K_x \end{bmatrix}$ can be calculated in a manner that the closed loop matrix system $(A - BK_c)$ is stable. The K_c matrix is obtained solving a cost-function minimization problem given by [29]:

$$J = \int_0^\infty \left((\vec{z})^T Q_k (\vec{z}) + \vec{\mu}^T R_k \vec{\mu} \right) \, dt \tag{29}$$

where $Q_k = Q_k^T \geq 0$, $R_k = R_k^T \geq 0$ and $\left(A, Q_k^{1/2} \right)$ are detectable.

Therefore, for a given state space LTI system, there is a gain matrix K_c which can minimize the cost function and bring all states (including the error) to zero simultaneously. The cost function minimization problem (Eq. (29)) can be solved using the Riccati equation [29].

3.3. Propeller Angular Speed

Using the control law described in section 3.2 represented by Eq.(29) the resultant thrust force (F_z) and the torques on three *BCS* directions (τ_x, τ_y and τ_z) are calculated for each time step. Therefore, the desired propeller angular velocities, which is actually the variable controlled on a real multi-copter, can be calculated from the control law output vector in order to keep the aircraft in balance and track the desired signal. Some works as [11] consider that the propeller angular velocities are the same for all n motors generating no torques around the CG, so the aircraft displacement on space relies only on the tilting mechanism, while the motor angular speed variation is used for height

tracking. However, the present work presumes that the propeller angular speed of each rotor can be estimated using the calculated input signal $\vec{u}(t)$. Thus, assuming stationary equilibrium condition, one can shows the actuation forces and moments can be written as:

$$\begin{bmatrix} \Delta F_z \\ \Delta \tau_x \\ \Delta \tau_y \\ \Delta \tau_z \end{bmatrix} = \begin{bmatrix} a_{11} & \cdots & a_{1i} \\ a_{21} & \cdots & a_{2i} \\ a_{31} & \cdots & a_{3i} \\ a_{41} & \cdots & a_{4i} \end{bmatrix} \begin{bmatrix} \Delta\Omega_1^2 \\ \vdots \\ \Delta\Omega_i^2 \end{bmatrix} \tag{30}$$

$$\vec{u}(t) = [A_m] \left[\Delta\Omega^2\right] \tag{31}$$

where the $[A_m]$ coefficients a_{ii} are obtained from the forces and moments equations (Eqs.(9) and (12)):

$$\begin{cases} a_{1i} = \cos\alpha_i \cos\beta_i k \\ a_{2i} = l \sin\gamma_i \cos\alpha_i \cos\beta_i k + z_{cg} \sin\beta_i k - b \sin\alpha_i \cos\beta_i \\ a_{3i} = -l \cos\gamma_i \cos\alpha_i \cos\beta_i k + z_{cg} \cos\beta_i \sin\alpha_i k + b \sin\beta_i \\ a_{4i} = -l \cos\gamma_i \sin\beta_i k + l \sin\gamma_i \sin\alpha_i \cos\beta_i k - b \cos\alpha_i \cos\beta_i \end{cases} \tag{32}$$

Hence, given the tilt angles α_i and β_i from Eqs. (23) and (24) and the desired control forces from Eq.(29), the angular velocities for the i^{th} motor propulsive group for each time step can be calculated using Eq.(31) and adding the nominal angular velocity for each rotor to maintain the multi-copter on hover condition ($\left[\Omega_0^2\right]$):

$$\left[\Omega^2\right] = [A_m]^{-1} \vec{u}(t) + \left[\Omega_0^2\right] \tag{33}$$

3.4. Control Architecture

Once the control law and inputs calculations were presented in sections 3.2 and 3.3, the control architecture used for the system to track a desired reference command (for instance a given trajectory on space) is presented on Fig.3.

From the figure, one can infer that the controller consists of two main blocks. One is the state regulator, which regulates the state feedback signal from the multi-copter plant ($\vec{x}$) multiplying it by the gain matrix K_x guaranteeing state stability. The second is the integral error control which receives the desired position reference signal for position ($\vec{r}$) and the desired tracking state signal (y_e). As presented previously in section 3.2 the number of integrators and K_p matrices is the same as the order of the reference signal differential equation [28] so that the tracking error for each state ($\vec{e}$) is driven to zero when $t \to \infty$. The computed forces and moments from the feedback stability are subtracted from the integral error control and, later, the tilting angles and propeller angular velocities model inputs are calculated using Eqs.(23), (24) and (33) serving as input to the multi-copter dynamical model represented by Eqs. (6) and (7).

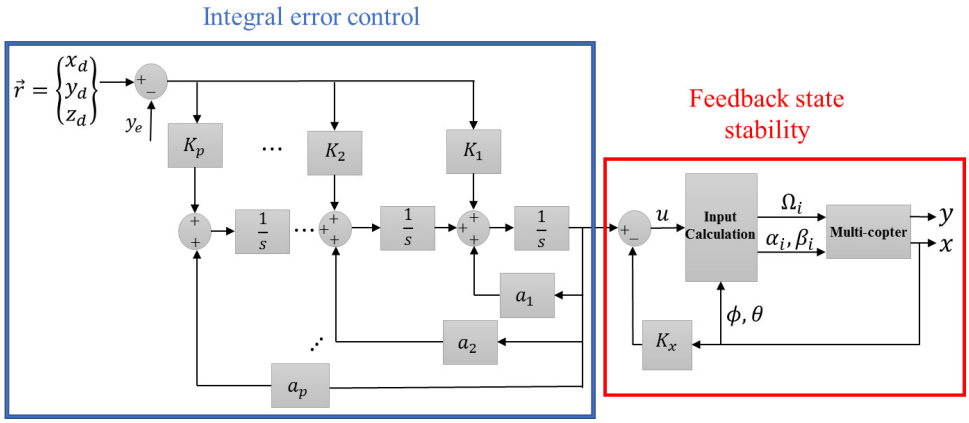

Figure 3: Servomechanism block diagram.

4. Numerical Simulations

This section deals with the numerical simulation of the closed loop tilting multi-copter model dynamics for trajectory following applications as previously illustrated in Fig. 3. From the results, it is expected to infer about the system stability and performance for different tilting configurations and mission tasks.

4.1. Simulation set up

To validate the dynamical model and the control law presented in Sections 2 and 3, respectively, a numerical simulation of the multi-copter platform was developed using a MATLAB/Simulink algorithm where the model equations and the control law architecture based on Fig. 3 were implemented and numerically simulated. Even though the control law was designed using the state-space linear model, simulations were performed using the non-linear dynamical equations from Section 2.

The main purpose of the simulations is to evaluate the system response for three different configurations: with longitudinal (α), lateral (β) and without (conventional fixed rotors) tilting mechanisms, considering different tracking scenarios or position reference input signals as: step and a waypoint trajectory estimated using fifth order polynomial equations.

Furthermore, for illustration, a quad-rotor MAV is used as case of study for the simulations containing the specific characteristics presented on Table 1. The properties were based on previous works from [24].

4.2. Step input

The first reference tested is a unitary step, which is mathematically represented by a first order differential equation ($\dot{r} = 0$, $a = 0$ and $p = 1$), in all three inertial directions x_E, y_E and z_E. Later, the feedback gain matrix are determined solving the minimization problem from Eq.(29). The solution results on two gain matrices (K_x and K_1 on Fig.3) once the reference is a first order derivative input signal.

Table 1: Quad-rotor properties.

Property	Parameter	Value	Unit [SI]
Number of rotors	n	4	-
Mass	m	0.620	kg
Inertia on x_b axis	J_{xx}	0.007	$kg.m^2$
Inertia on y_b axis	J_{yy}	0.007	$kg.m^2$
Inertia on z_b axis	J_{zz}	0.013	$kg.m^2$
Drag coefficient	k_d	4.8e-3	$N.s^2$
Arm Length	l	0.180	m
Thrust coefficient	k	8.901e-6	$N.s^2$
Propeller drag coefficient	b	1.1e-6	$N.m.s^2$

Figure 4 illustrates the x_E, y_E and z_E aircraft displacements for the three actuation mechanism configurations. From the figure, one can infer that the controller is able to converge the position error to zero and the Euler angles to the equilibrium position (hover condition) for the three configurations.

Notwithstanding, the system transient response differs from one to another considering that it has more oscillations on y_E direction when equipped with longitudinal tilting mechanism while it has a smother response with the lateral one. This behavior is also evidenced on the Euler angles transient response which, considering roll (ϕ) and pitch (θ) angles, the system with longitudinal tilting mechanism takes more time to converge to the equilibrium position.

Regarding the yawning angle (ψ), the oscillation amplitude is significantly higher for the multi-copter with the tilting mechanism. The fast convergence of the yaw angle for the lateral case can explains its lower overshoot on x_E and y_E directions once the mechanism makes the multi-copter easier to spin around the z_b axis (yaw movement) [24]. Finally, one can consider that the system response on z_E direction is the same for all three cases.

Figures 5, 6 and 7 present the system inputs (motor angular speed and tilt angle), calculated from Eq.(33), for the three configurations: no tilt, longitudinal

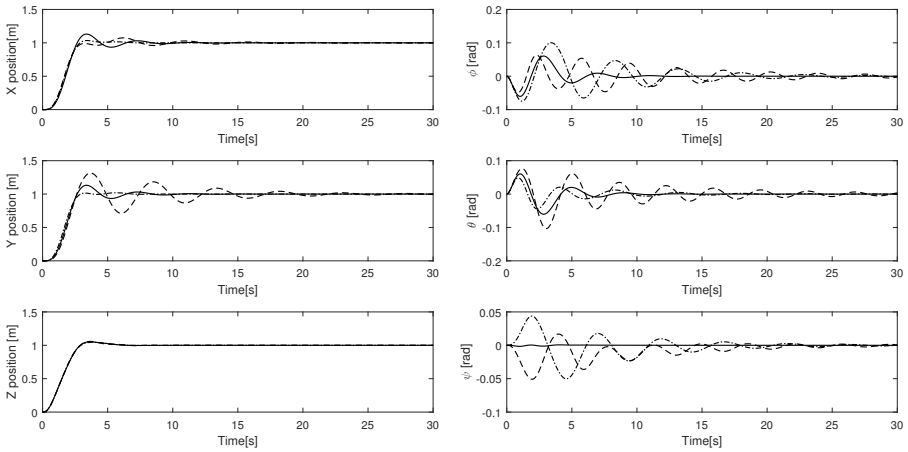

(a) (b)

Figure 4: Multi-copter position (a) and attitude (b) for three different configurations: longitudinal (- - -), lateral (-·-·-) and without tilting mechanism (——).

tilt and lateral tilt mechanism, respectively. Comparing the motor angular speed for each case, one can note that the addition of the tilt mechanism (Figs. 6(a) and 7(a)) to the system results on higher propeller angular speeds, i.e. the system spends more energy once the electric motor shaft speed is proportional to the electric current. Further, the motor input signal amplitude is almost the same for all four rotors, explaining the multi-rotor zero yaw angle through the simulation. On the other hand, the system with tilt mechanism oscillates in pairs, creating a resulting torque on z_b direction.

Moreover, on regarding the longitudinal and lateral tilting deflection angles on Figs. 6(b) and 7(b), it can be inferred that the system with longitudinal tilt mechanism has more oscillations and higher signal amplitude (0.1 *rad* or 6 *deg* approximately) compared to the lateral one (0.04 *rad* or 2.5 *deg* approximately). Consequently, the system is once again able to change its state with less tilt deflection, highlighting the lateral mechanism efficiency.

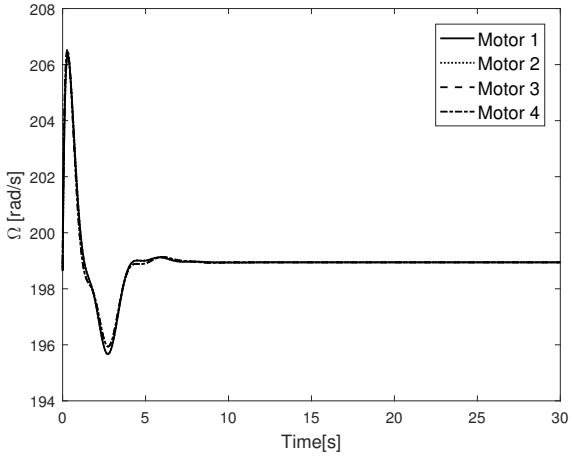

Figure 5: Multi-copter motor angular speed without tilting mechanism for step input.

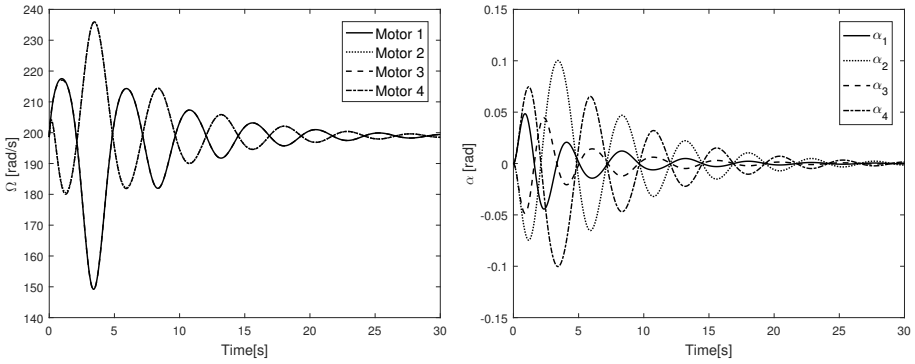

(a) (b)

Figure 6: Multi-copter motor angular speed (a) and tilt angle (b) for longitudinal tilting case for step input.

4.3. Waypoints Trajectory

In general, it is desired that the multi-copter is able to follow a predefined space trajectory passing through target waypoints.The aircraft trajectory optimization may be a cumbersome task considering that the system can be able to move from the point to another smoothly (low velocity and acceleration rates).

Hence, for the trajectory planning, fifth order polynomial curves can be used

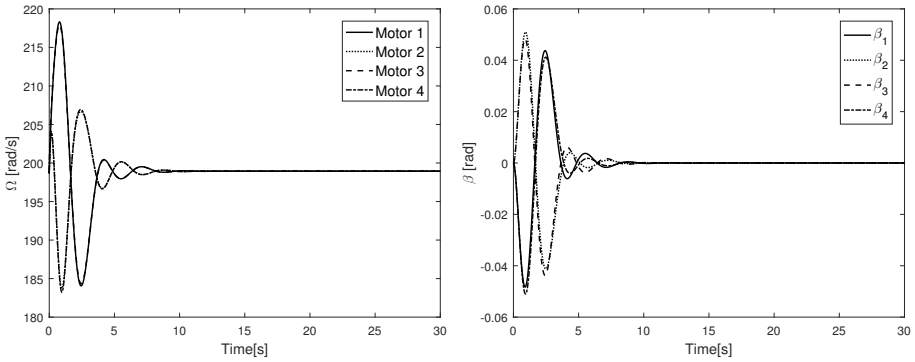

(a) (b)

Figure 7: Multi-copter motor angular speed (a) and tilt angle (b) for lateral tilting case for step input.

similarly as developed for robot manipulators in [30]. Following the proposed procedure, one can generate the x_E, y_E and z_E time-position curves, independently, for given position velocity and acceleration boundary restrictions. Then, the resulting polynomial curves are used as reference signal inputs (r_i) for the controller.

For instance, it is assumed a 3D trajectory passing through three desired positions: $\vec{r}_{des1} = [3 \quad 0 \quad 1]$, $\vec{r}_{des2} = [3 \quad 5 \quad 1]$ and $\vec{r}_{des3} = [0 \quad 5 \quad 1]$ as presented on Fig. 8. The three desired tracking points are interpolated using a fifth order polynomial resulting on three time-space curves represented by (——) on Fig. 9 (a). The flight path is expressed as fifth order polynomial curves, $p = 5$ on Eq.(26) and, consequently, the design controller contains five integrators and six gain matrices obtained from the Ricatti equation solution (Eq. (29)).

After performing the simulations, one can observe that the aircraft is able to follow the desired trajectory with minimal error for three motor configurations, as presented on Fig. 9 (a) where the four curves are superposed. Meanwhile, regarding the aircraft attitude (Euler angles) throughout its displacement on Fig.9 (b), it can be noted that the the system with the longitudinal tilting

mechanism has presented more oscillations on all three directions (roll, pitch and yaw) while they were attenuated considering the lateral tilting mechanism compared to the system without tilt mechanism.

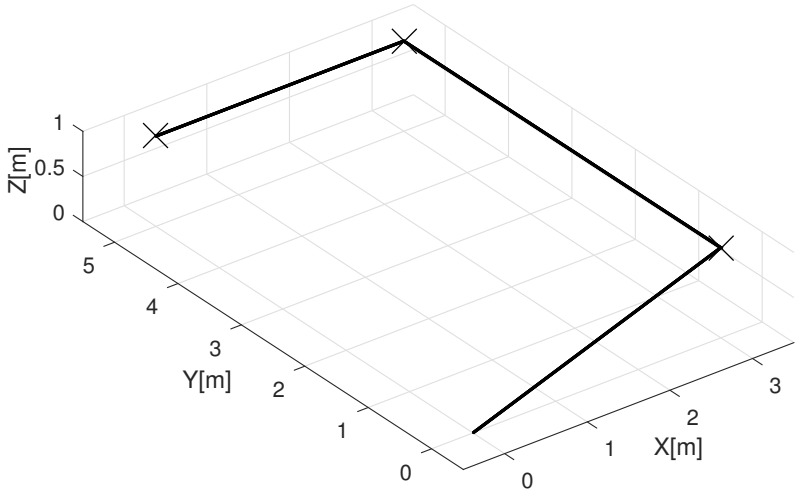

Figure 8: Generated 3D trajectory through desired points .

The motor angular speed for the requested trajectory for without, longitudinal and lateral tilting mechanism are presented on Figs. 10, 11 (a) and 12 (a), respectively. Regarding the first one, it can be concluded that the signal amplitude is almost the same for the four motors and, when looking closely at the signal, one can observe that the signal is rippled. This behavior can be explained by the solution of Eq.(33) and may have affect the system when applied on a real micro-controller.

Furthermore, once again, the signal amplitude for the tilting cases are higher and the signal amplitudes were different for each rotor resulting on a yawning moment. Also, the tilting angles for longitudinal directions (Fig. 11(b)) were higher compared to the lateral ones (Fig. 12(b)), pointing up the lateral tilting

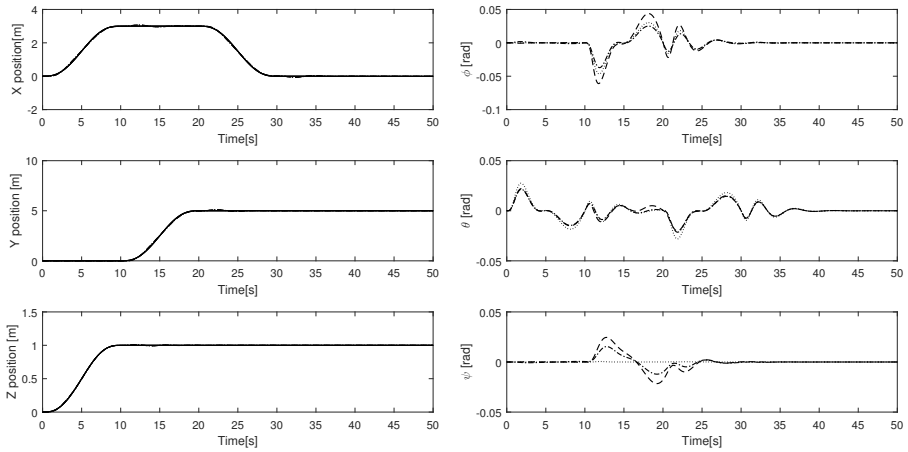

(a) (b)

Figure 9: Multi-copter position (a) and attitude (b) for a waypoint trajectory for three different configurations: longitudinal (- - -), lateral (-·-·-) and without tilting mechanism (·····). Reference position trajectory represented by (——) on (a).

mechanism control efficiency. Lastly, from Fig. 11(b), it can be observed that the tilting mechanisms actuates in pairs principally on the direction of the flight, i.e. 1 and 3 actuates more on the x_E direction and 2 and 4 on y_E direction for longitudinal case. The same pattern is noted when the system is endowed with lateral tilt mechanism (Fig.12(b)).

5. Conclusions

Considering the increasing demand for more versatile multi-copter MAVs in the past few years, many authors have proposed different actuation mechanisms to increase the system maneuverability and performance, and also solve the underactuation problem inherent to the system dynamics. Meanwhile, few investigations were done in order to evaluate the impact of the tilting mechanisms addition on the system stability and control effort for autonomous operations.

Hence, this work presented the dynamical modelling and trajectory con-

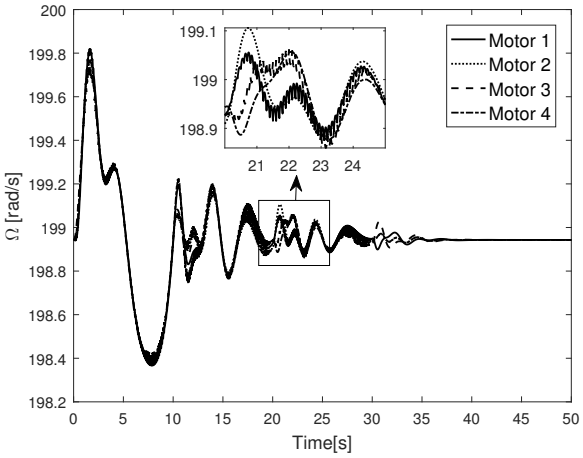

Figure 10: Multi-copter motor angular speed without tilting mechanism for waypoint trajectory.

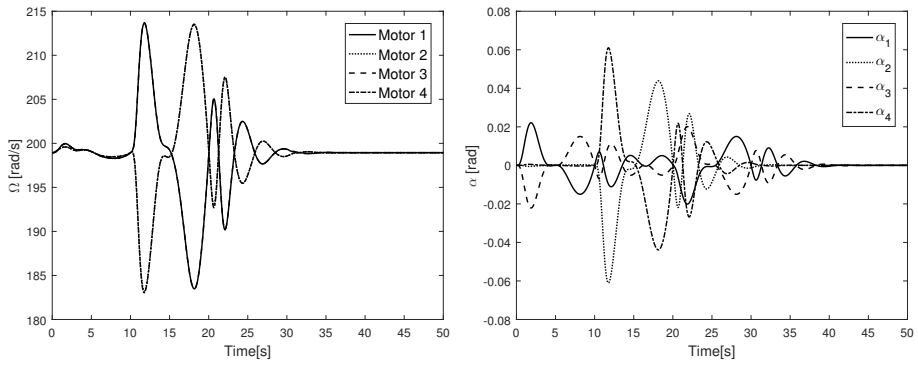

(a) (b)

Figure 11: Multi-copter motor angular speed (a) and tilt angle (b) for longitudinal tilting case for waypoint trajectory.

troller design for a generic multi-copter UAV endowed with a vectoring thrust mechanisms, either longitudinal or lateral. The proposed formulation can be applied on multi-copters containing n motor propulsive groups and/or tilting mechanisms with random structural arrangement which allows MAV designers to contemplate vectoring thrust mechanisms on their projects.

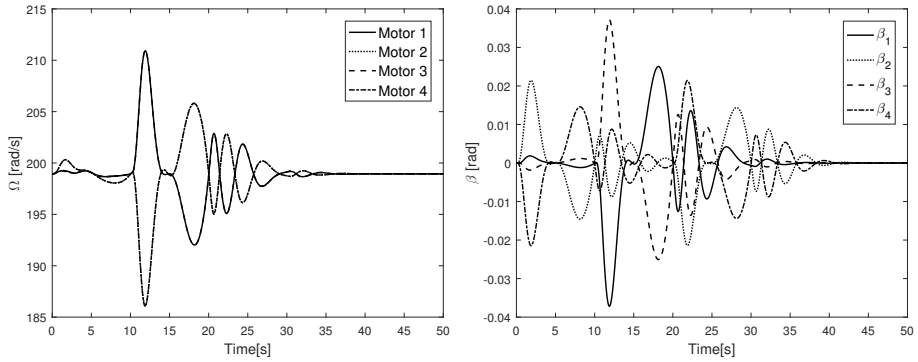

(a) (b)

Figure 12: Multi-copter motor angular speed (a) and tilt angle (b) for lateral tilting case for waypoint trajectory.

In order to perform autonomous operations, modern control techniques based on servomechanism design were applied in order to enable the aircraft to follow a desired space trajectory. The control structure considers a desired space position as input reference signal while the control law outputs are the required vertical force and torques. To acocmplish this, the proposed control system can be decomposed in two main parts: a servo tracking controller for command following containing as many integrators as the order of the reference input and a state feedback loop for stabilization. Later, the resulting control vector is used together with the system states to calculate the demanded motor angular velocity and tilt angles in order to keep the system stable.

The dynamical model and control law architecture were validated by Matlab/Simulink simulations for two different reference signal inputs: step (first order derivative equation) and a fifth order polynomial trajectory generated from desired target points (fifth order differential equations). From the simulations results, one can conclude that the control law was able to drive the system to the required desired position and to follow the reference trajectory with and without the tilting mechanism. However, the transient system responses were different for the three actuation scenarios. For instance, the system with longi-

tudinal tilt mechanism has presented higher amplitude oscillations on attitude which directly affects the trajectory following signal, as can be seen on Figs.4(a) and 4(b). The oscillations also made the motor angular velocities to have higher amplitudes. Meanwhile, the system endowed with longitudinal tilt mechanism had lower position oscillations (Figs.4(a)) highlighting its efficiency to control attitude, mainly the yaw angle.

Further, the system without tilting mechanism has presented lower motor angular velocities amplitude compared with the other two cases and, consequently, the system will spend less energy. Notwithstanding, for the waypoint trajectory, the motor angular velocity signal was rippled, which can harm the motor due to current oscillations. The observed behavior on the control inputs puts in check the usage of system endowed with tilting mechanisms for trajectory following.

For future work, other control techniques can be applied for the same problem as: backstepping, sliding-mode and heuristic techniques as neuro-fuzzy. Also, other formulations for the tilt-angle estimation can be tested, focusing on in-plane displacement. Finally, the control architecture can be tested on a real multi-copter UAV for validation of the model.

References

[1] S. Bouabdallah, Design and Control of Quadrotors With Application To Autonomous Flying, Master's thesis, École Polytechnique Fédérale De Lausanne, À La Faculté Des Sciences Et Techniques De L'Ingénieur, 2007.

[2] E. C. Suiçmez, Trajectory Tracking of a Quadrotor Unmanned Aerial Vehicle (UAV) VIA Attitude and position control, Master's thesis, Midle East Technical University, 2014.

[3] S. Bouabdallah, A. Noth, R. Siegwart, PID vs LQ control techniques applied to an indoor micro quadrotor, in: IEEE International Conference on Intelligent Robots and Systems (IROS), volume 3, Sendai, Japan, 2004, pp. 2451–2456.

[4] P. Castillo, S. Member, A. Dzul, R. Lozano, Real-Time Stabilization and Tracking of a Four-Rotor Mini Rotorcraft, IEEE Transactions on Control Systems Technology 12 (2004) 510–516.

[5] G. V. Raffo, M. G. Ortega, F. R. Rubio, Backstepping/nonlinear H control for path tracking of a quadrotor unmanned aerial vehicle, in: 2008 American Control Conference, Seattle, Washington, USA, 2008, pp. 3356–3361.

[6] D. Lee, H. J. Kim, S. Sastry, Feedback linearization vs. adaptive sliding mode control for a quadrotor helicopter, International Journal of Control, Automation and Systems 7 (2009) 419–428.

[7] K. Alexis, G. Nikolakopoulos, A. Tzes, Switching model predictive attitude control for a quadrotor helicopter subject to atmospheric disturbances, Control Engineering Practice 19 (2011) 1195–1207.

[8] R. Czyba, G. Szafranski, Control structure impact on the flying performance of the multi-rotor VTOL platform - Design, analysis and experimental validation, International Journal of Advanced Robotic Systems 10 (2013).

[9] B. J. Emran, A. Yesildirek, Robust Nonlinear Composite Adaptive Control of Quadrotor, International Journal of Digital Information and Wireless Communications 4 (2014) 213–225.

[10] E. J. Smeur, G. C. de Croon, Q. Chu, Cascaded incremental nonlinear dynamic inversion for MAV disturbance rejection, Control Engineering Practice 73 (2018) 79–90.

[11] S. Badr, O. Mehrez, A. E. Kabeel, A novel modification for a quadrotor design, in: 2016 International Conference on Unmanned Aircraft Systems, ICUAS 2016, IEEE, Arlington, VA USA, 2016, pp. 702–710.

[12] M. Cutler, N.-K. Ure, B. Michini, J. How, Comparison of Fixed and Variable Pitch Actuators for Agile Quadrotors, in: AIAA Guidance, Navigation, and Control Conference, Portland, Oregon USA, 2011, pp. 1–17.

[13] M. Ryll, H. H. Bülthoff, P. R. Giordano, Modeling and Control of a Quadrotor UAV with Tilting Propellers, in: IEEE International Conference on Robotics and Automation (ICRA), Saint Paul, Minnesota, USA, 2012, pp. 4606–4613.

[14] M. D. Hua, T. Hamel, C. Samson, Control of VTOL vehicles with thrust-tilting augmentation, Automatica 19 (2014) 2237–2244.

[15] A. Oosedo, S. Abiko, S. Narasaki, A. Kuno, A. Konno, M. Uchiyama, Large attitude change flight of a quad tilt rotor unmanned aerial vehicle, Advanced Robotics 30 (2016) 326–337.

[16] C. Hintz, C. Torno, L. R. Garc, Design and Dynamic Modeling of a Rotary Wing Aircraft with Morphing Capabilities, in: International Conference on Unmanned Aircraft Systems (ICUAS), Orlando, FL, USA, 2014.

[17] A. Nemati, M. Kumar, Modeling and Control of a Single Axis Tilting Quadcopter, in: American Control Conference (ACC), Portland, Oregon, USA, 2014, pp. 3077–3082.

[18] F. Kendoul, I. Fantoni, R. Lozano, Modeling and control of a small autonomous aircraft having two tilting rotors, Proceedings of the 44th IEEE Conference on Decision and Control, and the European Control Conference 2005 (2005) 8144–8149.

[19] E. Servais, B. D'Andrea-Novel, H. Mounier, Ground control of a hybrid tricopter, in: International Conference on Unmanned Aircraft Systems (ICUAS), Denver, Colorado USA, 2015, pp. 945–950.

[20] S. Salazar-Cruz, R. Lozano, J. Escareño, Stabilization and nonlinear control for a novel trirotor mini-aircraft, Control Engineering Practice 17 (2009) 886–894.

[21] J. Roskam, Airplane Flight Dynamics and Automatic Flight Controls, DARCorporation, Lawrence, KS, USA, 1979.

[22] K. P. Valavanis, Advances in Unmanned Aerial Vehicles, volume 33, Springer, 2007.

[23] H. Huang, G. M. Hoffmann, S. L. Waslander, C. J. Tomlin, Aerodynamics and control of autonomous quadrotor helicopters in aggressive maneuvering, in: IEEE International Conference on Robotics and Automation, 2009, pp. 3277–3282.

[24] F. M. M. Marques, Modeling, Simulation and Control of a Generic Tilting Rotor Multi-Copter, Master's thesis, Federal University of Uberlândia, 2018.

[25] B. Etkin, L. D. Reid, Dynamics of Flight Stability and Control, 3rd ed., John Wiley & Sons, INC, Toronto, 1996.

[26] A. S. Onen, L. Cevher, M. Senipek, T. Mutlu, O. Gungor, I. O. Uzunlar, D. F. Kurtulus, O. Tekinalp, Modeling and controller design of a VTOL UAV, in: 2015 International Conference on Unmanned Aircraft Systems, ICUAS 2015, Denver, Colorado USA, 2015, pp. 329–337.

[27] B. L. Stevens, F. L. Lewis, Aircraft Control and Simulation, John Wiley & Sons, INC, New York, NY, USA, 1992.

[28] E. Lavretsky, K. A. Wise, Robust and Adaptive Control, Advanced Textbooks in Control and Signal Processing, Springer London, London, 2013.

[29] R. S. Burns, Advanced Control Engineering, first ed., Butterworth Heinemann, Oxford, UK, 2001.

[30] J. J. Craig, Introduction to Robotics: Mechanics and Control, 3rd ed., Pearson;Prentice Hall, London, 2005.